Antiferromagnetism and ferromagnetism in layered $1T$-$CrSe_2$ with V and Ti replacements

Daniele C. Freitas,[1] Matías Núñez,[2,3,4] Pierre Strobel,[1] André Sulpice,[5] Ruben Weht,[6,7,2]
Armando A. Aligia,[8,2] and Manuel Núñez-Regueiro[1]

[1]*Institut Néel, Centre National de la Recherche Scientifique-Université Joseph Fourier 25 rue des Martyrs - BP 166, 38042, Grenoble cedex 9, France*

[2]*Consejo Nacional de Investigaciones Científicas y Técnicas, Buenos Aires, Argentina*

[3]*Instituto de Ciencias Básicas, Universidad Nacional de Cuyo, Mendoza, Argentina*

[4]*Departamento Materiales Nucleares, Centro Atómico Bariloche, Comisión Nacional de Energía Atómica, 8400 Bariloche, Argentina*

[5]*Institut Néel and CRETA, Centre National de la Recherche Scientifique-Université Joseph Fourier 25 rue des Martyrs - BP 166, 38042, Grenoble cedex 9, France*

[6]*Gerencia de Investigación y Aplicaciones, Comisión Nacional de Energía Atómica, Avda General Paz y Constituyentes, 1650 San Martín, Argentina*

[7]*Instituto Sabato, Universidad Nacional de San Martín y Comisión Nacional de Energía Atómica, 1650 San Martín, Argentina*

[8]*Centro Atómico Bariloche and Instituto Balseiro, Comisión Nacional de Energía Atómica, 8400 Bariloche, Argentina*

(Received 5 September 2012; revised manuscript received 30 November 2012; published 16 January 2013)

We have studied the effect of substitution of Cr in metastable $1T$-$CrSe_2$ by Ti and V on its structural and magnetic properties. The structural transitions observed between 165–180 K in the pure material are stomped by the doping. The pure compound has a magnetization corresponding to an antiferromagnetic (AF) ground state. On Ti substitution, we observe an increase of the lattice constants and a gradual passage towards a ferromagnetic state, while V replacement maintains AF order up to our highest doping, $x_V = 0.5$. With our experimental results and the help of first-principles calculations, we construct the phase diagram of the system.

DOI: 10.1103/PhysRevB.87.014420 PACS number(s): 75.50.Ee, 71.20.Be

I. INTRODUCTION

The discovery of superconductivity with high critical temperatures in iron pnictides[1] has added an important example of superconductivity issued from antiferromagnetic parent compounds of $3d$ transition metals (Cu[2], Ni[3], Co[4], Fe[1]). Most of such superconductors are unconventional, in the sense that the superconducting mechanism is believed not to be of the standard electron-phonon type. Moreover, they have a layered structure that yields two-dimensional properties that seem to be a necessary ingredient for high-temperature superconductivity. It is thus interesting to study what happens when antiferromagnetic states in other similar materials are destabilized by parameters such as doping. On the other hand, it is clear that superconductivity appears when the magnetic moment of the AF state is small, as in cuprates or iron compounds. Therefore possible candidates are low-spin chromium compounds. In the large family of 2D transition metal chalcogenides, only those based on chromium show antiferromagnetic ground states. One of the most interesting compounds is certainly $1T$-$CrSe_2$, a metastable material with the $Cd(OH)_2$ structure type, which has been synthesized through an indirect method[5] (see Fig. 1). Physical measurements show that the compound decomposes above 550 K and that the magnetic susceptibility is rather flat, with peaks at around 160 and 180 K, where abrupt changes of the a and c lattice parameters are observed. Band structure calculations showed that the ground state should be magnetic.[6] This result, combined with the weak temperature dependence of the measured magnetic susceptibility, indicates that an antiferromagnetic ordering occurs up to the decomposition temperature. Chemical substitution has significant influences on crystal structure, physical properties and electronic structure. In order to probe how the antiferromagnetic ground state is destabilized by hole doping, we performed partial substitution of Cr by V and Ti. We report here on the effect of these ion dopings on the structural and magnetic properties of $1T$-$CrSe_2$. We also present first-principles calculations that add to the experimental data in order to construct a phase diagram of the system. These are complemented by perturbative calculations in the Cr-Se hopping in which all correlations inside the Cr $3d$ shell are included. The paper is organized as follows. In Sec. II, we explain the synthesis of the samples, their characterization and how the magnetization is determined. Section III explains briefly the *ab initio* methods used to interpret the experimental results. In Sec. IV, we present these results. Section V contains the conclusion. The perturbative calculations are included in Appendix.

II. EXPERIMENTAL

The $1T$-$Cr_{1-x}V_xSe_2$ and $1T$-$Cr_{1-x}Ti_xSe_2$ compounds ($0 \leqslant x \leqslant 0.5$) were synthesized indirectly by oxidation of $ACr_{1-x}V_xSe_2$ and $ACr_{1-x}Ti_xSe_2$, A = K or Na. This method was used before by Van Bruggen *et al.*[5] to obtain $CrSe_2$ from K_xCrSe_2, $x \simeq 1$. The parent compounds were prepared by a molar mixture of the elements under argon atmosphere in a glove box. This mixture was then heated to the melting point of both, the alkaline and selenium, then kept at 700 °C for five days in an evacuated quartz tube. The tubes were opened in a glove box in order to prevent oxidation. The formation of the $A(Cr,M)Se_2$ (M = V or Ti) parent compound was confirmed by x-ray powder diffraction. Alkaline atom deintercalation was then carried out by reacting the parent compounds in solutions of iodine in acetonitrile. These suspensions were stirred for approximately 1 hour, using an excess of iodine. The final product was washed with acetonitrile to remove the iodide formed, filtered, and dried under vacuum. A mixture of

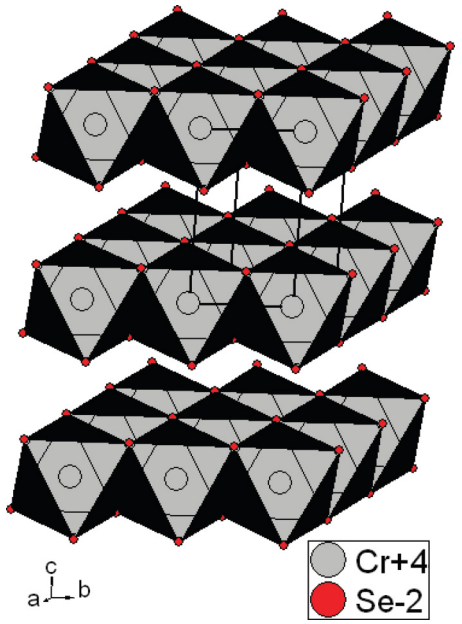

FIG. 1. (Color online) The schematic 3D structure of $1T$-$CrSe_2$. The selenium polyhedra centered on the metal ions are shown. The lines indicate the axes of the unit cell. This figure was generated by DIAMOND 2.1E[8] software.

brilliant dark gray platelets about 100 μm diameter and black powders with a metallic luster were obtained.

Samples were analyzed by energy dispersive x-ray spectroscopy in a Zeiss ultra field-emission gun scanning electron microscope operated at 20 kV. Twenty different points were measured from two different regions of the compounds compressed as rectangular bars.

Diffraction patterns of $1T$-$Cr_{1-x}V_xSe_2$ and $1T$-$Cr_{1-x}Ti_xSe_2$ were recorded at room temperature on a Bruker D8 diffractometer with Cu $K\alpha$ radiation and transmission geometry. Data were collected between $12^\circ \leqslant 2\theta \leqslant 95^\circ$, with a 0.025° step and acquisition times between 2 and 4 s per point. Lattice parameters (see Table I) were obtained by analysis of the peak positions by the CELREF program. Magnetization measurements were carried out in a METRONIQUE SQUID Magnetometer in the 1.8–300 K temperature range and a 0–7 T field range.

TABLE I. Lattice parameter of $1T$-$Cr_{1-x}V_xSe_2$ and $1T$-$Cr_{1-x}Ti_xSe_2$ obtained by analysis of the peak position by CELREF program.

Compound	a	c	c/a
$CrSe_2$	3.3931	5.9218	1.74525
$Cr_{0.9}V_{0.1}Se_2$	3.3906	5.9204	1.74612
$Cr_{0.88}V_{0.12}Se_2$	3.3881	5.9518	1.75668
$Cr_{0.8}V_{0.2}Se_2$	3.3828	6.0077	1.77595
$Cr_{0.7}V_{0.3}Se_2$	3.3733	6.0342	1.78881
$Cr_{0.6}V_{0.4}Se_2$	3.3719	6.0627	1.79801
$Cr_{0.5}V_{0.5}Se_2$	3.3713	6.0772	1.80263
$Cr_{0.9}Ti_{0.1}Se_2$	3.411	5.9348	1.7399
$Cr_{0.8}Ti_{0.2}Se_2$	3.4289	5.9414	1.73274
$Cr_{0.7}Ti_{0.3}Se_2$	3.4316	5.953	1.73476
$Cr_{0.6}Ti_{0.4}Se_2$	3.4566	5.9501	1.72137
$Cr_{0.5}Ti_{0.5}Se_2$	3.4638	5.948	1.71719

III. THEORETICAL

The energetics of the different magnetic structures were investigated by electronic structure calculations within the framework of the Density Functional Theory (DFT).[9] To do that, we used mainly the QUANTUM ESPRESSO code,[10] which uses a plane-wave basis to describe the electronic wave functions and ultrasoft pseudopotentials to represent the interaction between electrons and ions.[11] The exchange and correlation potential was considered at the level of the Generalized Gradient Approximation (GGA) based on the Perdew-Burke-Ernzerhof (PBE) expression.[12] Results using the Local Density Approximation (LDA)[13,14] were conceptually similar showing only minor differences in the energetics. A simple orthorhombic supercell with 12 atoms was used for our calculations (see inset in Fig. 11), similar to a previous work by Fang and coworkers,[6] exploring several antiferromagnetic configurations. Reciprocal space integrations were performed on a $(8 \times 8 \times 8)$ Monkhorst-Pack mesh.[15] As $CrSe_2$ has a metastable structure, the lattice parameters and the position of the Cr atoms were kept fixed at the experimental values, while the Se atoms were allowed to relax until forces on each atom were below 0.002 eV/Å. To corroborate our results, some calculations were crosschecked with the WIEN2K package.[16] These *ab initio* calculations were complemented by strong coupling calculations, explained in Appendix, which start from the exact eigenstates of isolated $Cr4$ and include Cr-Se hopping as a perturbation.

IV. RESULTS

A. Structural characterization

The diffractograms are shown in Fig. 2. All compounds crystallize in the $Cd(OH)_2$ structure type (space group $P\bar{3}m1$, No. 164). In this structure, the transition metal M and Se atoms occupy the Wyckoff positions a (cell origin) and d =(1/3, 2/3, z) with $z \simeq 0.25$, respectively. The M atoms are octahedrally coordinated by selenium and form hexagonal layers sandwiched between two layers of Se atoms (see Fig. 1). The different panels of Fig. 3 show the variation of the lattice parameters as a function of doping, x, for the $1T$-$Cr_{1-x}V_xSe_2$ and $1T$-$Cr_{1-x}Ti_xSe_2$ systems. The lattice parameter for the end members $1T$-$TiSe_2$ and $1T$-VSe_2 were taken from Wiegers.[7]

In the vanadium case, a and c vary in opposite directions, whereas in the titanium case, both cell parameters increase with doping. In both cases, Vegard's law is approximately verified for the variation of a (i.e., bond lengths in the layers). The variation of c, however, is not linear: the slope of $c(x)$ tends to decrease for high c values. This may be related to difficulties in achieving high-doping levels, especially, in the titanium system, where the $x = 0.5$ sample was found to contain about 15% of a $TiSe_2$ impurity phase and has probably an actual doping content lower than the nominal one. Although an ionic model is not strictly applicable to selenides, it is interesting to note that the ionic radius of Cr^{4+} is closer to the V^{4+} one than the Ti^{4+} one. Accordingly, the variation of a is much smaller in the vanadium case (-1.3%) than in

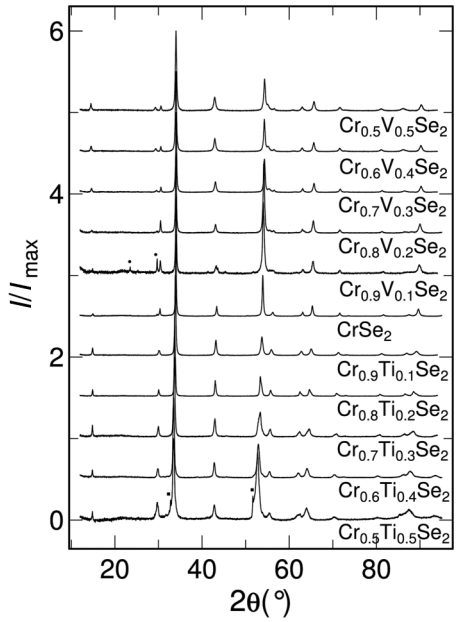

FIG. 2. X-ray powder diffractograms of the $1T$-$Cr_{1-x}V_xSe_2$ and $1T$-$Cr_{1-x}Ti_xSe_2$ compounds. For better visualization, the intensities of the peaks were normalized by the largest peak and the diffractograms were displaced on the vertical scale by 0.5 for each compound. Circles (squares) mark $TiSe_2$ (Se) impurity peaks.

the titanium one (+4%). On the other hand, the presence of vanadium affects more strongly the c parameter, and this is illustrated by the variation of c/a (see Fig. 4). In the $Cd(OH)_2$ structure, the coordination of the M atom is known to be an ideal octahedron when $c/a = 1.633$ and $z = 0.250$, and the octahedron tends to be trigonally distorted for large c/a.[7] Figure 6 shows that $c/a > 1.633$ in both systems, but that vanadium doping increases this ratio, i.e., increases the M site distortion, whereas titanium doping decreases it slightly. Assuming $z \simeq 0.250$, this is consistent with the fact that Ti^{4+} has an isotropic d^0 electron configuration, whereas V^{4+} is a d^1 ion known to induce distortions in its coordination sphere.

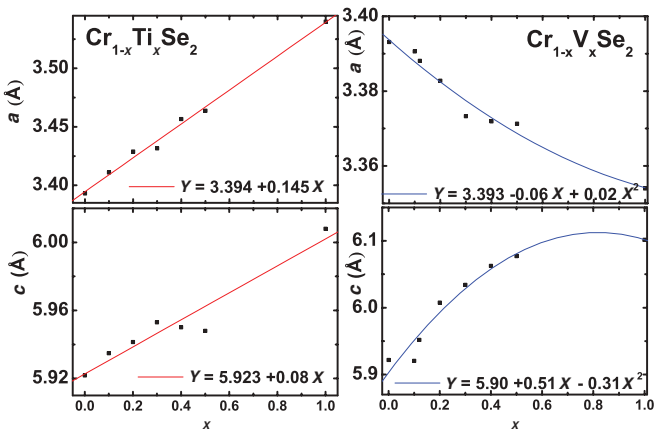

FIG. 3. (Color online) The lattice parameter as a function of the concentration of Ti, x, for $1T$-$Cr_{1-x}Ti_xSe_2$ (left) and of V, x, for $1T$-$Cr_{1-x}V_xSe_2$ (right) obtained by analysis of the peak position by CELREF program.

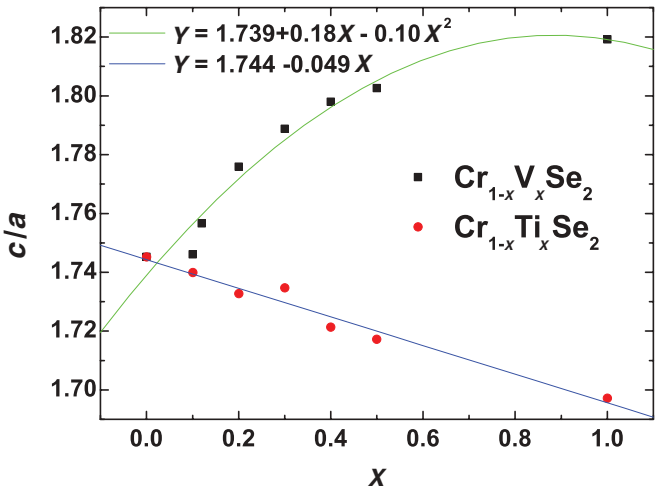

FIG. 4. (Color online) Ratio of lattice parameters c/a for $Cr_{1-x}V_xSe_2$ and $Cr_{1-x}Ti_xSe_2$ compounds as a function of the concentration of V and Ti, respectively. The coordination of the metal is an ideal octahedron for $c/a = 1.633$ and $z = 0.250$.

B. Temperature dependence of the lattice parameters

As reported by van Bruggen *et al.*,[5] there is a crystallographic transition involving a shortening of the c axis at low temperatures. In reality, there are two that influence noticeably the magnetization, as indicated by the two anomalies observed in the magnetization of the pure compound. It was proposed that this transition is due to a clustering of the Cr atoms. In the pure compound (circles in Fig. 5), we observe that the c parameter increases as the temperature is lowered till around 180 K, where a sudden contraction occurs. According to van Bruggen *et al.*,[5] in the high-temperature phase of $CrSe_2$ above 180 K, with only short-range order of the Cr clusters, an adequate stacking of the randomly buckled $CrSe_2$ sandwiches is not possible. Thus the c axis in the high-temperature phase will be larger and will increase with increasing (short-range order) metal clustering going to lower temperatures. At the phase transition near 180 K, a sudden decrease of c is observed, as in the low-temperature phase an adequate stacking of the buckled sheets is possible due to the onset of long-range order. Curiously, the anomaly in the a parameter appears at lower temperatures, 160 K. Both anomalies have a clear effect in the magnetization, as seen in Fig. 6. We observe that the effect of the V or Ti replacement is strong on the temperature dependence of the c parameter. There is almost no c axis contraction and only the rate of increase diminishes. This is compatible with the previous interpretation, i.e., the impurities cause a disorder in the buckling, that impedes the adequate nesting of the planes, and the sudden contraction. It is difficult to determine precisely where the long-range order establishes, presumably it may be broadened over a large temperature interval. On the other hand, the transition in the a parameter, which corresponds to a small increase of a, becomes undetectable with the lowest replacement. As a consequence of both behaviors, a broadening of the magnetization anomalies due to these transitions is expected, as seen in Fig. 6.

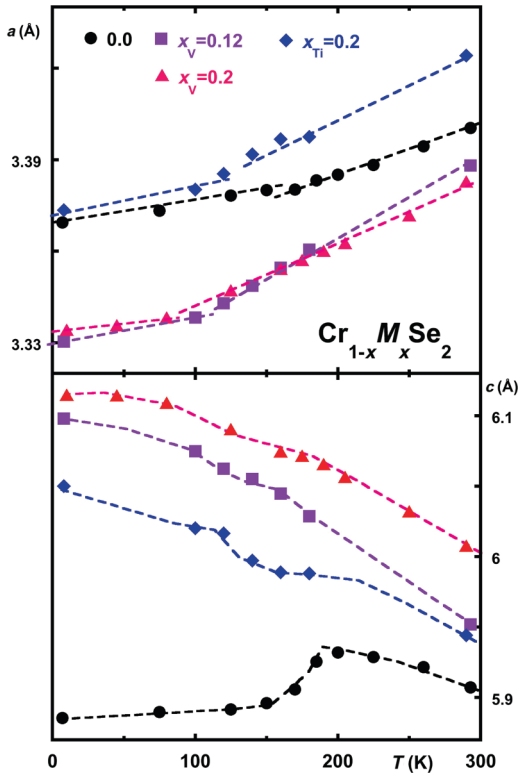

FIG. 5. (Color online) Lattice parameter as a function of temperature for several $Cr_{1-x}M_xSe_2$ (M = V or Ti) samples. Pure compound (circles), V concentration is 0.12 (squares), V concentration is 0.2 (riangles), and Ti concentration is 0.2 (diamonds).

C. Energy dispersive x-ray spectroscopy

The nominal stoichiometry was approximately obtained to both series compounds. The $Cr_{0.5}Ti_{0.5}Se_2$ was not homogeneous, there were regions with $TiSe_2$ and $CrSe_2$ that led to difficulties of analyzing the composition of this compound. We found small quantities of Na or K atoms in all the compounds suggesting that the deintercalation was not completed. This value grows for the largest replacement of Ti atoms, about 4% for the $Cr_{0.5}Ti_{0.5}Se_2$ and 2% for the $Cr_{0.6}Ti_{0.4}Se_2$. For the other compounds it was about 1%.

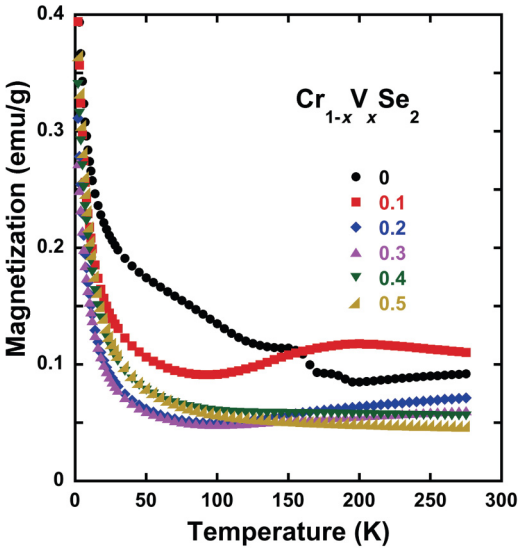

FIG. 6. (Color online) Magnetization of $Cr_{1-x}V_xSe_2$ over an applied field of 1 T. Zero-field-cooling (ZFC) and FC curves show practically no difference. The structural transitions are clearly seen on the undoped curve and as a smooth anomaly in the doped ones.

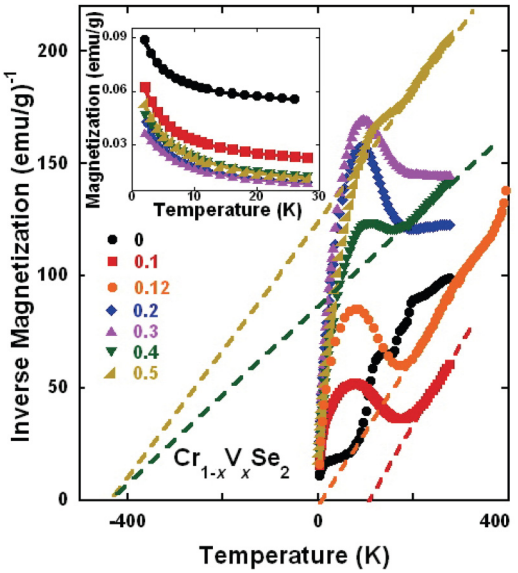

FIG. 7. (Color online) Inverse magnetization of $Cr_{1-x}V_xSe_2$ samples at $0.1T$. At high concentration, the high-temperature behavior shows clearly a Curie law with high and negative asymptotic Curie constant, that we call θ_N, meaning strong antiferromagnetic interactions within the planes. (Inset) Fit of Curie-Weiss law to the magnetization FC of $Cr_{1-x}V_xSe_2$ at low temperature.

D. Magnetization

Figure 6 displays the magnetization versus temperature curves under an applied field of 1 T for $Cr_{1-x}V_xSe_2$. The pure compound shows a magnetization similar to that of Ref. 5 and the value of susceptibility that we extract from our measurements at 1 T is roughly that reported. At low temperature, the magnetization curve of the $Cr_{1-x}V_xSe_2$ compounds can be fitted by the Curie's law (see Fig. 7), with the parameters shown in Table II. From the Curie constant C, we can extract the number of ions in the paramagnetic state through the expression:[17] $C = N(p\mu_B)^2/(3k_B)$, where N is the number of atoms by volume unit, $p = 2\sqrt{S(S+1)}$ supposing that the orbital moment is quenched, μ_B and k_B

TABLE II. Curie constant and Curie temperature of $Cr_{1-x}V_xSe_2$ obtained by the fit at low temperature of Curie-Weiss law [$M = M_0 + C/(T-\theta)$] to the magnetization curves. See Fig. 7.

Compound	C (10^{-3} emu K/g Oe)	θ (K)	M_0
$CrSe_2$	0.157	−2.1	0.0500
$Cr_{0.9}V_{0.1}Se_2$	0.195	−2.3	0.0170
$Cr_{0.8}V_{0.2}Se_2$	0.181	−2.4	0.0037
$Cr_{0.7}V_{0.3}Se_2$	0.226	−4.3	0.0019
$Cr_{0.6}V_{0.4}Se_2$	0.286	−4.7	0.0041
$Cr_{0.5}V_{0.5}Se_2$	0.279	−3.5	0.0031

have the usual meaning, assuming only Cr^{+4} ions. We found that for the pure compound, about 8% of the Cr^{+4} ions are in the paramagnetic state and are most probably interstitial atoms. For the $Cr_{1-x}V_xSe_2$ compounds, there are about 5% of these ions. On high vanadium substitution (see Fig. 6), the paramagnetism of the samples is reduced. Although VSe_2 has a temperature independent Pauli-like susceptibility, a combination of both behaviors cannot explain the observed low magnetization. Rather, vanadium substitution seems to have a strong effect on the ground state. From electronic band structure calculations, the antiferromagnetic order of $CrSe_2$ is seemingly of itinerant type and as such it should be very sensitive to the defects that are present in our samples. Isolated vanadium atoms, with local magnetic moments, act as stabilizers for the itinerant antiferromagnetic ground state, decreasing the low-temperature magnetization. In fact, if they did not interact with the AF ground state, the low-temperature Curie tail of the samples should be proportional to vanadium concentration. Our Curie fits (inset of Fig. 7) on the low-temperature behavior yield a Curie "constant" weakly varying with vanadium concentration, with a Curie temperature, denoting antiferromagnetic interactions. Thus it is clear that the moments are "absorbed" into the AF order and are not free magnetic moments, since they do not contribute to the Curie law. For low V substitution, the samples show below room temperature a very small magnetization compatible with systems in an AF ordering. The inverse magnetization plot, Fig. 7, shows that the highly substituted samples, follow a Curie law at high temperatures, with a negative Curie temperature, implying strong AF interactions in the planes. Around the crystallographic transition, the samples show a decrease of the magnetization, followed at lower temperatures by the Curie tail of paramagnetic impurities. For these samples, it seems then that the crystallographic transition triggers the full AF ordering and may be associated to a Néel temperature.

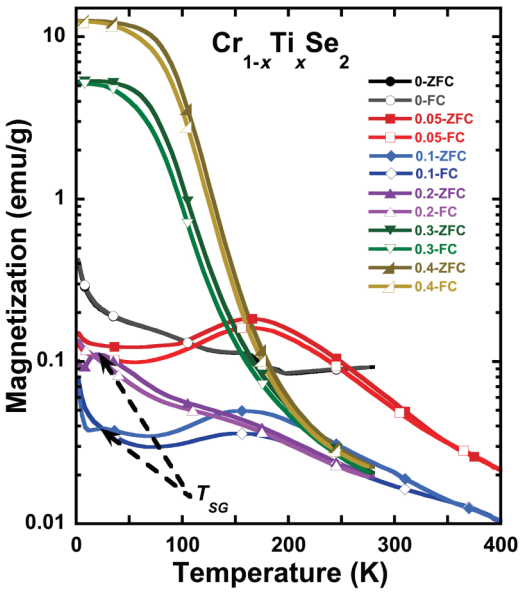

FIG. 8. (Color online) Magnetization ZFC (full symbols) and FC (empty symbols) of $Cr_{1-x}Ti_xSe_2$ over an applied field of 0.1 T. The vertical axis is in logarithmic scale.

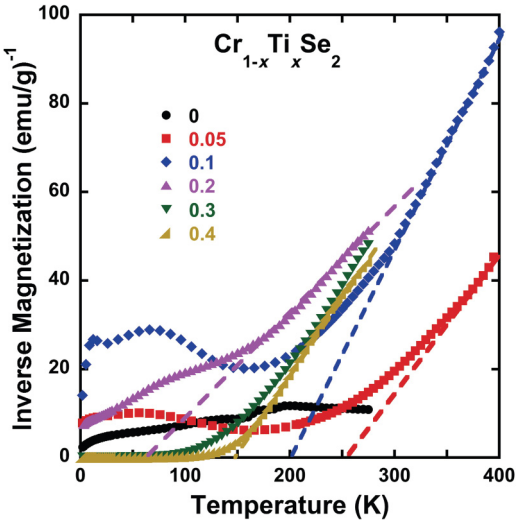

FIG. 9. (Color online) Inverse magnetization of $Cr_{1-x}Ti_xSe_2$ samples at $0.1T$. The high-temperature behavior shows clearly a Curie law with positive asymptotic Curie constant, meaning strong ferromagnetic interactions within the planes. At low temperatures for small x, there is an AF ordering of the planes, while for large x, the ordering is clearly ferromagnetic.

Titanium substitution should introduce a gradual decrease of the magnetization, as expected for the introduction of defects that carry a +4 charge and no magnetic moment. The analysis of the low-temperature behavior (see Fig. 8) confirms this point of view for $x_{Ti} \leqslant 0.2$, as there is no substantial variation of the low-temperature Curie constant, i.e., the number of paramagnetic impurities (presumably intercalated Cr ions), is roughly independent of the Ti concentration. For a doping value higher than 0.2, the compounds show a ferromagnetic behavior (See Figs. 8 and 9). Ti substitution increases the lattice parameter a, which favors ferromagnetic interactions in the plane, as reported on several Cr layered systems,[6] e.g., misfit CrS_2[20] and $Na_xCr_xTi_xS_2$.[21]

V. DISCUSSION

Studies of the Cr-Se-Te system with different types of replacements have followed the evolution of AF (in Se based compounds) towards F (in Te based materials).[24–29] From our measurements, we can construct a similar phase diagram corresponding to both the Ti and V replacement. Both replacements expand the c parameter but the ratio c/a decreases (approaching the value corresponding to ideal $CrSe_6$ octahedra) with Ti substitution and increases with V substitution (see Figs. 3 and 4). Starting with the pure material, as we replace Cr with Ti, as c/a decreases, the ferromagnetic (F) interactions override the antiferromagnetic (AF) ones. At low Ti concentration, we obtain samples that order below $T_N \sim 200$ K into a low magnetization state, presumably antiferromagnetic. The high-temperature Curie plot yields, however, a positive and high Curie temperature, as for a ferromagnet (See Fig. 9). This is usually observed in layered compounds with competing AF and F interactions, e.g., F ordering within the planes but AF coupling between

the planes (AF2), as observed in $TlCrSe_2$[18] or AF ordering in the plane and F ordering between planes (AF3). (See inset in Fig. 13.) As the distribution of Ti atoms is not necessarily homogeneous at atomic level, some competition between AF and F interactions is expected, that can explain the spin-glass cusp at low temperatures, denoted by T_{SG} in Fig. 8. With higher Ti content, the system shifts to an F ordering, while conserving the spin-glass cusp. The Ti region of this diagram is typical to what is observed in systems with competing F and AF interactions.[19]

On V replacement, there is a slight contraction of the lattice parameter a and a more important expansion of c with the result that c/a increases (see Fig. 4) and the AF interactions are enhanced. We continue to observe a low magnetization state below $T_N \sim 200$ K with a high-temperature Curie constant that remains positive, but decreases and tends to zero for $x = 0.12$. At high V concentration, the magnetic ordering remains always around $T_N \sim 200$ K, but now the Curie temperature becomes negative, θ_N, as determined from our high-temperature data. At high V replacement then, we have AF ordered planes that also interact AF between each other, as symbolized by the $AF1$ structure inserted in Fig. 13, which is the magnetic structure theoretically proposed before for $CrSe_2$.[6]

There are two main complications for our synthesis, both due to the defects inherent to these samples. In the first place, the de-intercalation method that we have used, creates stacking faults, as seen from the single crystal x-ray patterns that we have obtained. However, they will not affect the in-plane interactions, although they will render long-range magnetic orderings more difficult, broadening the transition temperatures. The second type of defects are the inevitable intercalated chromium ions, consequence of the existence of a large number of Cr_xSe_y phases with related structures,[22,23,25] where $1 \leqslant y/x \leqslant 2$. Once more, these defects will mainly affect the interplane interactions and the long-range ordering, but to a minor extent the in-plane physics.

In order to see the effect of the change of the lattice parameters on the relative stability of the different magnetic phases, we have performed first-principles calculations for the three antiferromagnetic orderings, i.e., AF1, AF2, and AF3, and the F phases. These are the simplest collinear ordered arrangements, although more complex, e.g., helicoidal,[34] can also be possible. To this end, we used the unit cell of the $CrSe_2$ without any actual cation substitution but with the experimental cell parameters, relaxing only the Se atoms. The resulting differences of energy of the AF phases with respect to the F one is shown in Fig. 10. According to our calculations, AF3 is the lowest energy state up to about $x = 0$, and then the system switches to a F configuration. The trend follows the one observed experimentally in general. The negative θ_C observed at high V concentration is compatible with both, an AF1 ground state, or an AF3 one in which the AF interactions are larger than the F ones. The major discrepancy with theory is that for $x_{Ti} \leqslant 0.2$, the ground state is AF and not F. The difference might be due to the effects of real cation substitution or to the interstitials present in the sample, if we assume that they increase the AF coupling between the planes. Thus they would favor AF1 with respect to AF3 at high V concentration and AF2 with respect to F at low Ti concentration. In fact, our calculations for $Cr_{0.5}V_{0.5}Se_2$ (see

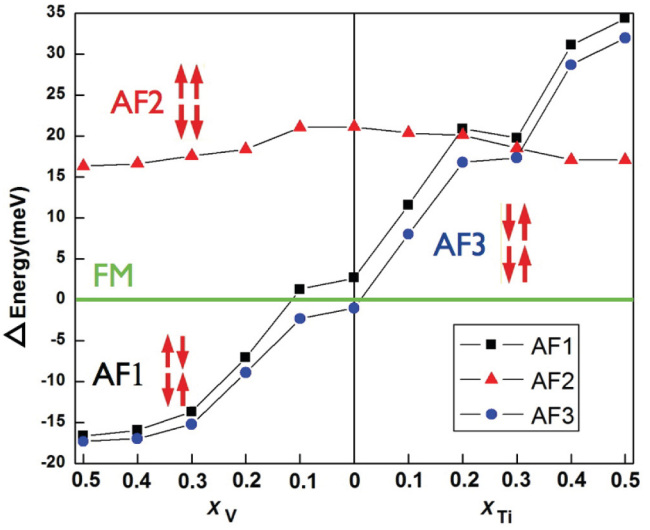

FIG. 10. (Color online) Evolution of the energies of the different antiferromagnetic phases referred to the energy of the ferromagnetic ordering obtained from first-principles calculations. Lattice parameters were taken from the experimental results shown in Table. I. At each point, the cell parameters were kept fixed as well as the Cr positions, while the Se atoms were allowed to relax.

Fig. 11) demonstrate that V substitution clearly favors an AF ordering.

Starting from the undistorted $CrSe_2$ and keeping a constant, we have made a uniform compression or dilation of the unit cell in the z direction, changing the value of c (see Fig. 11). The difference of energy between the AF and F phases decreases almost linearly with increasing c. In particular, for the compressed structure that corresponds to perfect $CrSe_6$ octahedra $c/a = 1.633$, the F order is stabilized by an energy

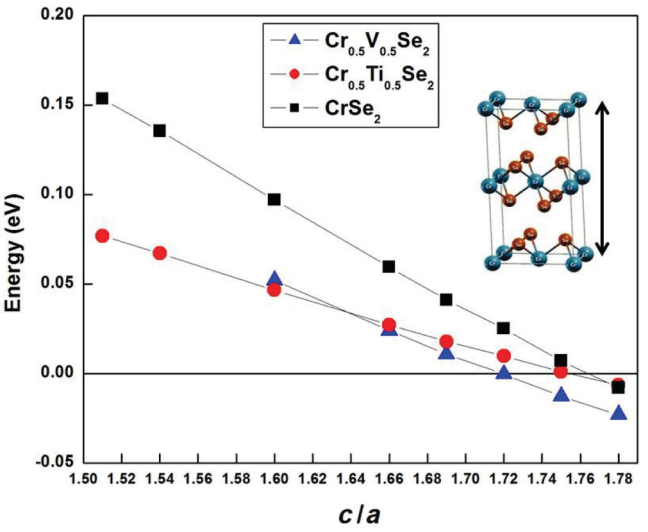

FIG. 11. (Color online) The stability of the AF3 phase with respect to the F phase is investigated varying the ratio of lattice parameters c/a keeping a fixed. The difference in energy between both phases (energy per formula unit) is plotted above. Results for pure $CrSe_2$ are shown as well as the effect of real doping with V and Ti corresponding to cases $Cr_{0.5}V_{0.5}Se_2$ and $Cr_{0.5}T_{0.5}Se_2$, respectively.

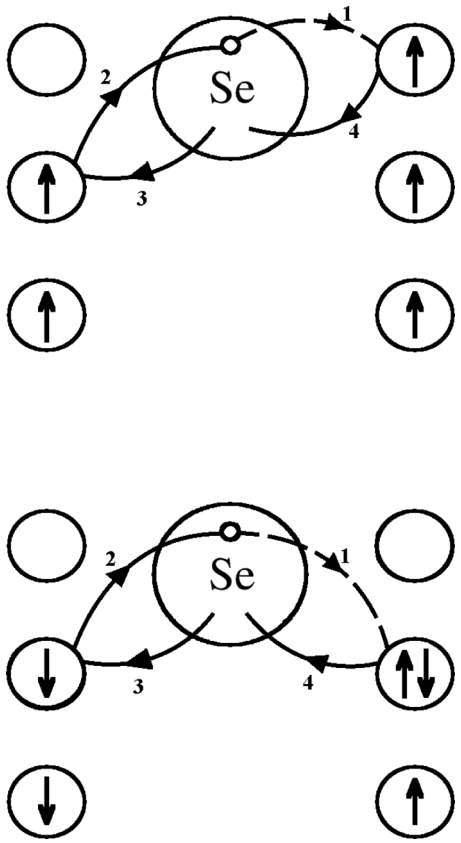

FIG. 12. Scheme of an intermediate virtual state after the first step (dashed line) in the calculation of the effective exchange between $S = 1$ Cr states in fourth-order perturbation theory. The small circles represent the three t_{2g} orbitals of two nearest Cr atoms. The circles at the top represent $xy + xz + yz$ orbitals of higher energy, which are unoccupied in the ground state of Cr^{+4}. (Top) An electron from Se jumps to the unoccupied orbital $xy + xz + yz$. (Bottom) An electron from Se jumps to an occupied orbital. The remaining hopping processes are indicated by full lines.

near 0.06 eV per Cr atom. The addition of V or Ti atoms in the supercell reduces this value and accelerates the transition to the AF phase for increasing c/a.

These calculations point out that c/a is the most relevant parameter that determines the nature of the magnetic interactions. This can be understood in a localized picture as follows. For isolated regular $CrSe_6$ octahedra, and in a system of axis pointing to the Se atoms, the t_{2g} orbitals xy, yz, zx are degenerate, and two of them with the same spin are occupied in Cr^{+4} according to Hund's rules. The $S = 1$ spin states of neighboring $CrSe_6$ octahedra (which share two Se atoms in common) interact with an effective exchange interaction J_{eff}, which can be calculated in fourth-order perturbation theory in the Cr-Se hopping (for example, a hole jumps from a Cr atom to Se, then to another Cr and comes back, see Fig. 12). This hopping is similar to that of cobaltates and is illustrated, for example, in Fig. 1 of Ref. 30. Similar arguments apply if direct Cr-Cr hopping is included.

The different contributions to J_{eff} include intermediate states with one Cr^{+3}, which can be classified in two groups: (1) Cr^{+3} has one electron in each t_{2g} orbital (top of Fig. 12) and (2) Cr^{+3} has one doubly occupied t_{2g} orbital (bottom of Fig. 12). In the group 1, F contributions dominate, because Cr^{+3} with total spin $S = 3/2$ is favored by Hund's rules, leading to smaller denominators. Instead, all contributions of group 2 are AF because starting from two Cr^{+4} $S = 1$ ions with the same spin projection, it is not possible to doubly occupy any orbital because of Pauli principle. They have also larger denominators because they involve excited Cr^{+3} states. Thus one might expect F ordering for undistorted octahedra. When c/a is increased from the ideal value 1.633, the degeneracy of the t_{2g} orbitals is broken and the state $xy + yz + zx$ is split from the other two linear combinations. If it lies higher in energy, the F contributions of group 1, which necessarily occupy it, decrease in magnitude, and AF order is favored, in agreement with the *ab initio* calculations. We have made the perturbative calculations confirming these expectations for reasonable values of the parameters. The details are in Appendix.

Taking into consideration the observed AF and F ground states, the magnitudes of the measured θ_C and θ_N together with the energy calculations, we can propose the phase diagram shown on Fig. 13. At high V concentration, the experimental results are consistent with an AF phase, either AF1 or AF3. The latter is favored by our first-principles calculations, but the difference of energy between both phases is small. According to the measured θ_C, the ground state corresponds to the AF3 phase below $x_V = 0.1$. A AF3 is also probably the ground state at low Ti concentration, which, by continuity, suggests that it may also be the ground state of the pure $1T$-$CrSe_2$. The slight increase of θ_C at $x_{\text{Ti}} = 0.05$, may signal the passage towards a ferromagnetic configuration in the planes and then a AF2 ground state, before becoming totally F at high Ti concentration. The AF2 phase is a common ground state for several Cr layered materials.[18] Neutron scattering measurements are planned to verify this phase diagram.

The fact that "hole" doping, i.e., the decrease of the total number of electrons in the system with Ti (V) substitution, is secondary to the effect of distortion of the lattice on the magnetic properties, is against an exclusively itinerant view of magnetism in the system. The best way to test the effect of hole doping would be by intercalation of electronegative ions, that would strongly modify the electron count, with feeble structural effects. Unfortunately, all our attempts in that sense have been unsuccessful. The question of the interaction between the structural phase transition and the magnetic ordering remains open.

VI. CONCLUSION

We have studied the effect of substitution of Cr in metastable $CrSe_2$ by Ti and V on its structural and magnetic properties. The former increases the basal parameter, while the latter decreases it. The contraction of the c parameter at 180 K and the anomaly in the a parameter at 165 K in the pure material become both undetectable with the lowest substitution. The pure compound has a magnetization corresponding to an antiferromagnetic (AF) ground state. On Ti substitution, we observe a gradual passage towards a ferromagnetic state, while V replacement maintains AF up to our highest doping, $x_V = 0.5$. The phase diagram compounded by our first-principles and many-body calculations, confirms

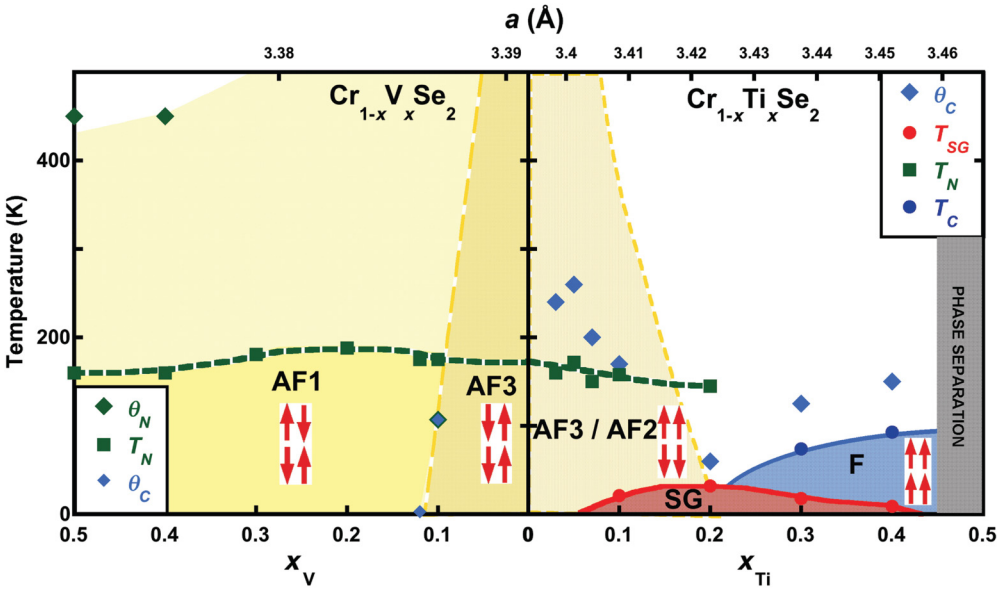

FIG. 13. (Color online) Phase diagram for V and Ti chromium replacement in $CrSe_2$. θ_N is $-\theta_C$ as obtained from the inverse magnetization. T_N is the apparent Néel temperature, where the magnetization decreases with decreasing temperature. T_C is determined as the maximum in the derivative of the magnetization with respect to temperature. Reduction of c/a by Ti substitution shifts the system towards ferromagnetism, while increasing c/a by V substitution favors antiferromagnetism. The transition at $x_V \approx 0.1$ is well defined by $\theta_C = 0$ while in the region of $0 \leqslant x_{\rm Ti} \leqslant 0.2$ both AF2 and AF3 are possible.

that the nature of the magnetic interactions is determined by the ratio of lattice parameters c/a.

ACKNOWLEDGMENTS

D.C.F. gratefully acknowledges support from the Brazilian agencies CAPES and Cnpq. This work was partially supported by the project TetraFer ANR-09-BLAN-0211 of the Agence Nationale de la Recherche of France, and Grants PIP Nro 11220080101821 and 11220080100047 of CONICET-Argentina, Grants PICT R1776, PICT PRH 0102 and PICT 837/07 of the ANPCyT-Argentina, and Research Poject 06/M048 of SeCTyP-Argentina. We acknowledge clarifying discussions with J-L. Tholence and C. Lacroix. We are grateful to S. Pairis, P. Toulemonde, and O. Leynaud for technical help.

APPENDIX: CALCULATION OF THE EFFECTIVE EXCHANGE IN THE Cr PLANES BY PERTURBATIONS IN THE Cr-Se HOPPING

Here we describe the calculation of the effective exchange $J_{\rm eff}$ in the planes in fourth-order perturbation theory in the Cr-Se hopping t. For simplicity, we start considering perfect $CrSe_6$ octahedra and write the $3d$ t_{2g} orbitals of Cr and $4p$ orbitals of Se in a system of reference where x, y, and z point in the Cr-Se directions. The main symmetry axis of the structure (the crystallographic direction c) is the direction (1,1,1) in this system of coordinates. The effect of the elongation of the octahedra is included in an increase Δ in the energy of the orbital $c = (xy + yz + zx)/\sqrt{3}$, which points along the crystallographic direction c.

The Hamiltonian is $H = H_0 + H_t$. The unperturbed Hamiltonian can be written as

$$H_0 = \sum_i \left[\epsilon_{\rm Cr} \sum_{\alpha\sigma} n_{i\alpha\sigma} + \Delta \left(\sum_{\sigma} d^\dagger_{ic\sigma} d_{ic\sigma} \right) + H^i_I \right] + \epsilon_{Se} \sum_{j\gamma\sigma} n_{j\gamma\sigma}, \tag{A1}$$

where i (j) runs over the Cr (Se) sites of the planes, $n_{i\alpha\sigma} = d^\dagger_{i\alpha\sigma} d_{i\alpha\sigma}$, $d^\dagger_{i\alpha\sigma}$ creates an electron in the t_{2g} orbital α (xy, yz or zx) with spin σ at site i. Similarly, $n_{j\gamma\sigma} = p^\dagger_{j\gamma\sigma} p_{j\gamma\sigma}$, and $p^\dagger_{j\gamma\sigma}$ creates an electron at the corresponding Se site. H^i_I contains the interactions at the Cr site i and can be written in the form[31]

$$H^i_I = U \sum_{\alpha} n_{i\alpha\uparrow} n_{i\alpha\downarrow} + \frac{1}{2} \sum_{\alpha\neq\beta,\sigma\sigma'} (U' n_{i\alpha\sigma} n_{i\beta\sigma'} + J d^\dagger_{i\alpha\sigma} d^\dagger_{i\beta\sigma'} d_{i\alpha\sigma'} d_{i\beta\sigma}) + J \sum_{\alpha\neq\beta} d^\dagger_{i\alpha\uparrow} d^\dagger_{i\alpha\downarrow} d_{i\beta\downarrow} d_{i\beta\uparrow}, \tag{A2}$$

where $U' = U - 2J$.

The perturbation is

$$H_t = t \sum_{\langle ij\rangle\alpha\gamma} \epsilon_{ij\alpha\gamma} (d^\dagger_{i\alpha\sigma} p_{j\gamma\sigma} + \text{H.c.}), \tag{A3}$$

where $\epsilon_{ij\alpha\gamma} = \pm 1$ or 0 depending on the Cr-Se direction and the symmetry of the orbitals, as discussed previously for the cobaltates.[32,33]

The calculation of $J_{\rm eff}$ is similar to that of the superexchange in the cuprates and can be regarded as a four-step process in which one hole at a Cr site jumps to Se, then to another Cr site and the same hole or another one of the latter site comes back to the original Cr site. In the electron language, these processes

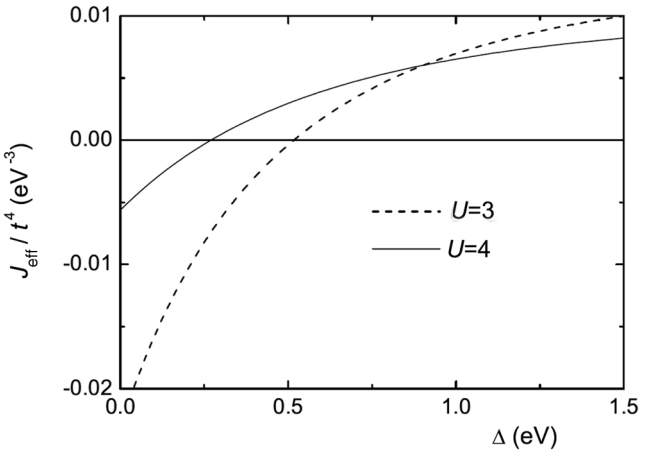

FIG. 14. Effective exchange between $S = 1$ Cr^{+4} spins in the plane as a function of the splitting between $xy + yz + zx$ and doubly degenerate e_i orbitals, for $G = 2$ eV, $J = 0.7$ eV, and two different values of U.

are represented in Fig. 12. The difference with the cuprates is the multiorbital character of the transition metals. The ground state of Cr^{+4} is a spin triplet, and for positive Δ, as we consider here, the occupied orbitals are $e_1 = (2xy - yz - zx)/\sqrt{6}$ and $e_2 = (zx - yz)/\sqrt{2}$.

It can be easily checked that H_I^i is invariant under orthogonal O(3) transformations. Using this fact for the transformation that maps (c,e_1,e_2) onto (xy,zx,yz), respectively, we can borrow the results of Ref. 31 for the energies of the different excited states that enter the perturbative expressions. We neglect the terms which involve two holes in the Se atom, because they involve an extra cost in Cr-Se charge-transfer energy and Cr Coulomb repulsion U. Adding all remaining contributions, we obtain after a rather lengthy but straightforward algebra:

$$\begin{aligned}\frac{J_{\rm eff}}{t^4} = &-\frac{4}{27}\frac{1}{(G+\Delta)^2(U-3J+\Delta)}\\ &+\frac{4}{27}\frac{1}{(G+3J+\Delta)^2(U+\Delta)}\\ &+\frac{5}{9}\frac{1+\Delta/r}{(G+4J+\Delta-r)^2(U+J+\Delta-r)}\\ &+\frac{5}{9}\frac{1-\Delta/r}{(G+4J+\Delta+r)^2(U+J+\Delta-r)},\end{aligned} \quad \text{(A4)}$$

where $G = 2U - 4J + \epsilon_{\rm Cr} - \epsilon_{\rm Se}$ is the charge-transfer energy and $r = (\Delta^2 + J^2)^{1/2}$.

Taking $J = 0.70$ eV obtained from the fit of atomic energy levels, and choosing $G = 2$ eV, the resulting effective exchange in the planes is represented in Fig. 14 for two different values of U. One can see that while $J_{\rm eff}$ is negative for undistorted octahedra, as the splitting Δ between c and e_n states increases, $J_{\rm eff}$ increases and changes sign. This is in agreement with the *ab initio* results for increasing ratio of the lattice parameters c/a.

[1] Y. Kamihara, T. Watanabe, M. Hirano, and H. Hosono, J. Am. Chem. Soc. **130**, 3296 (2008).
[2] J. G. Bednorz and K. A. Muller, Z. Phys. B **64**, 189 (1986).
[3] T. Watanabe, H. Yanagi, T. Kamiya, Y. Kamihara, H. Hiramatsu, M. Hirano, and H. Hosono, Inorg. Chem. **46**, 7719 (2007).
[4] K. Takada, H. Sakurai, E. Takayama-Marumachi, F. Izumi, R. A. Dilanian, and T. Sasaki, Nature (London) **422**, 53 (2003).
[5] C. F. Van Bruggen, R. J. Haange, G. A. Wiegers, and D. K. G. De Boer, Physica B **99**, 166 (1980).
[6] C. M. Fang, C. F. Van Bruggen, R. A. de Groot, G. A. Wiegers, and C. Haas, J. Phys.: Condens. Matter **9**, 10173 (1997).
[7] G. A. Wiegers, Physica B **99**, 151 (1980).
[8] G. Bergerhoff, M. Berndt, and K. Brandenburg, Res. Natl. Inst. Stand. Technol. **101**, 221 (1996).
[9] P. Hohenberg and W. Kohn, Phys. Rev. **136**, B864 (1964).
[10] P. Giannozzi *et al.*, J. Phys.: Condens. Matter **39**, 395502 (2009).
[11] D. Vanderbilt, Phys. Rev. B **41**, 7892 (1990).
[12] J. P. Perdew, K. Burke, and M. Ernzerhof, Phys. Rev. Lett. **77**, 3865 (1996).
[13] J. P. Perdew and A. Zunger, Phys. Rev. B **23**, 5048 (1981).
[14] D. M. Ceperley and B. J. Alder, Phys. Rev. Lett. **45**, 566 (1980).
[15] H. J. Monkhorst and J. D. Pack, Phys. Rev. B **13**, 5188 (1976).
[16] P. Blaha, K. Schwarz, G. K. H. Madsen, D. Kvasnicka, and J. Luitz, WIEN2K (Technische Universitt Wien, Austria, 2002).
[17] C. Kittel, *Introduction to Solid State Physics*, 5th ed. (Wiley, New York, 1976).
[18] S. Ronneteg, M-W. Lumey, R. Dronskowski, and R. Berger, J. Alloys Compd. **403**, 71 (2005).
[19] J. L. Tholence, F. Holtzberg, T. R. McGuire, and S. von Molnar, J. Appl. Phys. **52**, 7350 (1979).
[20] A. Lafond, A. Meerschaut, J. Rouxel, J. L. Tholence, and A. Sulpice, Phys. Rev. B **52**, 1112 (1995).
[21] P. Colombet and L. Trichet, Solid State Commun. **45**, 317 (1983).
[22] Y. Adachi, M. Ohashi, T. Kaneko, M. Yuzuri, Y. Yamaguchi, S. Funahashi, and Y. Morii, J. Phys. Soc. Jpn. **63**, 1548 (1994).
[23] T. Kaneko, J. Sugawara, K. Kamigaki, S. Abe, and H. Yoshida, J. Appl. Phys. **53**, 2223 (1982).
[24] M. Yuzuri and K. Segi, Physica B **86-88**, 891 (1977).
[25] M. Yuzuri, J. Phys. Soc. Jpn. **35**, 1252 (1973).
[26] S. Ohta, Y. Narui, and Y. Sakayori, J. Magn. Magn. Mater. **170**, 168 (1997).
[27] J. Wontcheu, W. Bensch, S. Mankovsky, S. Polesya, H. Ebert, R. K. Kremer, and E. Bruecher, J. Solid State Chem. **181**, 1492 (2008).
[28] J. Wontcheu, W. Bensch, S. Mankovsky, and S. Polesya, Prog. Solid State Chem. **37**, 226 (2008).
[29] Z-L. Huang, W. Bensch, D. Benea, and H. Ebert, J. Solid State Chem. **178**, 2778 (2005).
[30] A. A. Aligia and T. Kroll, Phys. Rev. B **81**, 195113 (2010).
[31] A. A. Aligia and M. A. Gusmão, Phys. Rev. B **70**, 054403 (2004).
[32] W. Koshibae and S. Maekawa, Phys. Rev. Lett. **91**, 257003 (2003).
[33] A. Bourgeois, A. A. Aligia, T. Kroll, and M. D. Núñez-Regueiro, Phys. Rev. B **75**, 174518 (2007).
[34] F. M. R. Engelsman, G. A. Wiegers, F. Jellinek, and B. Van Laar, J. Solid State Chem. **6**, 574 (1973).